Opinion | Vol. 12, No. 2 / 1 Feb 2022 / Optical Materials Express 524

Optical Materials EXPRESS

Lithography-free metamaterial absorbers: opinion

AMIR GHOBADI,[1,2] TURKAN GAMZE ULUSOY GHOBADI,[1] AND EKMEL OZBAY[1,2,3,4,*]

[1]NANOTAM - Nanotechnology Research Center, Bilkent University, Ankara 06800, Turkey
[2]Department of Electrical and Electronics Engineering, Bilkent University, Ankara 06800, Turkey
[3]UNAM–National Nanotechnology Research Center, Bilkent University, Ankara 06800, Turkey
[4]Department of Physics, Bilkent University, Ankara 06800, Turkey
[*]ozbay@bilkent.edu.tr

Abstract: Although advancement in nanofabrication provides the opportunity to realize nanoscale geometries with high resolutions, the scalability and repeatability issues limit their large-scale applications. Lithography-free metamaterial absorbers (LFMAs) are a potential route for the upscaling of these designs. With restricted freedom in their synthesis, the importance of the proper material choice is emphasized. Herein, we provide a comprehensive overview of the recently developed LFMAs, from both design and material perspectives, while considering their most promising applications.

1. Routes and materials

Light confinement and harvesting in dimensions much smaller than the wavelength have been the subject of many studies in the field of metamaterial-based perfect absorbers. Metals, at sub-wavelength dimensions, can undergo strong light-matter interaction in a broad spectral range [1]. This happens through the collective oscillation of free conduction electrons, so-called localized surface plasmon resonance (LSPR), or inter-band transitions. However, the realization of plasmonic nano units requires complex and large-scale incompatible routes such as lithography-based techniques. Therefore, recently, the concept of lithography-free metamaterial absorbers (LFMAs) has attracted intensive attention [2,3]. The most common type of these scalable LFMAs is planar multilayer designs, with the dominant absorption mechanism of Fabry-Perot (FP) resonance modes [2]. Metal-insulator-metal (MIM) and MIM-insulator (MIMI) and periodic $(MI)_N$ cavity configurations are the most common cavity absorbers. One-dimensional photonic crystal (1D-PC) based configurations are also utilized to achieve light absorption in ultrathin absorbing layers. Nanostructured LFMAs could outweigh these planar designs, especially in applications where both strong absorption and high active surface area are desired. Recently, several innovative fabrication routes have been developed to meet this requirement. Deposition induced structuring [4,5], dewetting induced nanounit formation [6–8], oblique angle deposition of three-dimensional (3D) structures [9–14], direct laser writing [15], template-assisted etching [16,17], and deposition [18,19] are examples of these methods, as shown in Fig. 1. Aside from the importance of the route, the choice of the right material is another prominent factor in LFMA design. Figure 2 outlines the most suitable materials for the building of LFMAs. In the ultraviolet (UV) and visible, a vast variety of semiconductors and metals can be used to achieve this goal. To extend this functionality toward longer ranges such as near-infrared (NIR) and short-wavelength infrared (SWIR), lossy metals such as Ti, Cr, W, and Bi could be utilized in a proper configuration [2]. Moreover, doped metal oxides such as Al-doped ZnO (AZO) [20], Ga-doped ZnO (GZO) [21], In-doped SnO_2 (ITO) [22], In-doped CdO (ICO) [23,24], and Ce-doped In_2O_3 (CIO) [25] that show epsilon-near-zero (ENZ) characteristics in the SWIR range could be used in LFMAs. Metal nitrides such as TiN, ZrN, HfN, and InN could also

#448363
Journal © 2022

https://doi.org/10.1364/OME.448363
Received 10 Nov 2021; accepted 15 Nov 2021; published 13 Jan 2022

Optical Materials EXPRESS

reveal a plasmonic response in the infrared (IR) range [26–29]. Moreover, these alternative plasmonic materials show tunable plasma frequency in the mid-wavelength infrared (MWIR) range. In longer wavelengths (i.e. MWIR, long-wavelength infrared (LWIR), and far-infrared (FIR)), LFMAs can be realized through the excitation of i) optical phonon in metal oxides [30], ii) plasmonics in highly doped semiconductors [31], iii) plasmonic resonances in two dimensional (2D) materials such as graphene and black phosphorus (BP) [32,33], and iv) phonon polariton modes in polar materials [34].

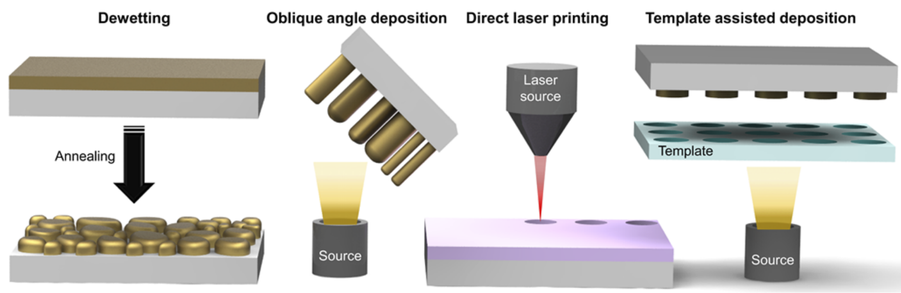

Fig. 1. Schematic illustration of lithography-free fabrication routes.

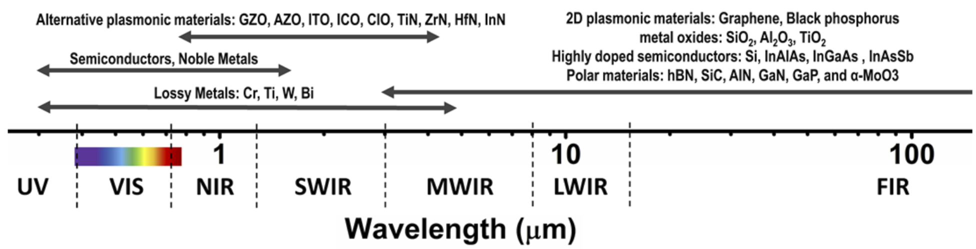

Fig. 2. Possible absorber materials for the realization of LFMAs in different portions of the optical spectrum.

2. Applications

LFMAs are divided into two material categories: i) metallic and ii) non-metallic. Their applications are sorted based on their operational wavelength range; i) sun blackbody radiation spectrum (sun-BBRS) or so-called solar spectrum covering UV-visible-NIR-SWIR ranges, and ii) earth blackbody radiation spectrum (earth-BBRS) covering SWIR-MWIR-LWIR-FIR.

2.1. Sun-BBRS

Metallic LFMAs. Planar metallic LFMAs can reveal spectrally selective narrowband or broadband light absorption. The narrowband planar LFMAs are commonly utilized in color filtering applications [35]. While simple MIM cavity design can generate additive red-green-blue (RGB) colors in transmissive mode (with amplitudes much below unity), tandem shape cavity architectures can generate high-efficiency RGB colors in reflection mode [36–40]. These planar LFMAs can also show dynamically tunable color generation, through the change in spacer layer index or thickness. For index modulation, phase change materials (PCMs) such as GST [41,42], VO_2 [43], Sb_2S_3 [44], or even Sb [45] can be used as the spacer to generate thermally tunable colors. For nanoscale thickness tuning of the spacer, swelling/deswelling of humidity-sensitive polymers and hydrogels is employed to fabricate dynamic MIM color filters [46–48]. Besides filtering, the narrowband LFMAs have potential application in colorimetric sensing platforms such as bio-, and gas-sensing, where the external stimuli shifts the resonance peak of the LFMA [12,49,50]. However, in sensing, a high surface area is desired to maximize the interaction of light with the surrounding environment. Thus, nanostructures such as dewetted or oblique angle deposited plasmonic units offer higher sensitivities [51,52].

On the other side, the broadband LFMAs can harvest a large portion of the solar spectrum, which is desired for photoconversion applications. In metals, photoconversion functionality can be acquired using the excitation and extraction of energetic hot electrons. However, due to the femtosecond relaxation of hot electrons with a dominant mechanism, called Landau damping, only energetic carriers can traverse the Schottky barrier [53]. This photoemission efficiency is even less in planar and large particle sizes [54] where absorption is due to non-resonant inter-band transitions rather than the LSPRs. Despite intensive efforts to find alternative high performance and low-cost plasmonic elements such as Al [55–57], conductive oxides [27,58,59], transition metal nitrides/carbides (such as TiN) [60,61], and doped semiconductors [62–64], the efficiency of hot electron designs is still low. The same obstacles are present in the hot electron based photodetection and photoelectrochemical water splitting (PEC-WS) applications [65]. The alternative route is to use these metallic LFMAs in the application platforms where metals are not the photoactive layer such as thermal photovoltaic (TPV) and steam generation. In TPV, a broadband LFMA absorbs photons, transforms them into heat, and reradiates it using a selective emitter with a spectral emission peak overlapping with the PV bandgap. Based on theoretical calculations, a solar TPV, with an ideal design of absorber and emitter, can achieve efficiencies exceeding the Shockley-Queisser limit [66]. The narrowband emitter can also be realized with a multilayer dielectric-based 1D-PC design, making the overall system a lithography-free architecture [67]. Solar-driven steam generation is another promising area for broadband LFMAs. Advancements in this area have proven efficiencies as high as 90% at 4-sun intensity ($4\,\mathrm{kW\,m^{-2}}$) [68]. Different from TPV, in this application, a high area is a must to maximize the heat transfer between the LFMA and water.

Non-metallic LFMAs. Similar to metallic ones, the dominant application of non-metallic LFMAs in sun-BBRS is photoconversion and semiconductors are its main building blocks [69]. In most semiconductors, the carrier diffusion length is much shorter than the light penetration depth. Therefore, the bulk recombination of carriers limits their efficiency. However, sub-wavelength semiconductor-based LFMAs can offer optically thick, electrically thin platforms suitable for photoconversion systems, such as PV, photodetection, and PEC-WS [67]. Planar metal-semiconductor (MS) and metal-dielectric-semiconductor (MDS) cavity designs are proven to achieve near-unity absorption in deep sub-wavelength semiconductor thicknesses [70–80]. In 2D monolayer semiconductors, dielectric-based 1D-PC and Bragg reflector designs are the right strategy to confine the entire power in the position of the 2D layer and efficiently harvest it [81–83]. Besides the optical response, the electrical characteristics of these semiconductors are also a prominent factor that affects the performance outcome. Ideally, a crystalline semiconductor film should be grown in ultrathin dimensions, but it is a challenging task. The transfer of external crystalline thin films [79,84] and the CVD growth of 2D semiconductors can provide high-quality thin films. In PEC-WS, two more factors should be adopted in the design of these LFMAs; i) surface area and ii) long-term structural integrity (or stability) of the photoelectrode [69]. While planar LFMAs have already been used as photoanode and photocathode components in PEC-WS [84,85], nanostructured designs with a higher water-semiconductor interface can improve the activity. To have a high surface area with good crystallinity, template-assisted etching of crystalline semiconductor host seems a promising approach [16]. A thin protection layer with proper band alignment could be utilized to solve the stability issue.

2.2. Earth-BBRS

Metallic LFMAs. In most metals, the LSPR excitation and interband transition happen in the UV-visible range. However, lossy metals in $(MI)_N$ and metal-1D-PC configurations, can reveal resonant light absorption in the SWIR-LWIR range [37,86–89]. These planar absorbers can act as selective/broadband thermal emitters with possible applications in radiative cooling and thermal camouflage [90–93]. Integration of these LFMAs with PCMs offers dynamically tunable IR emitters/absorbers [94–96]. Such a design could even enable passive radiative thermostat functionality by adjusting the visible and IR absorption/emission [97].

Non-metallic LFMAs. Highly doped semiconductors, doped metal oxides, metal nitrides/carbides, and 2D materials such as graphene, and BP are alternative plasmonic materials in MWIR, LWIR, and FIR range [34]. Heavily doped semiconductors such as Ge, Si, III-V compounds are appealing alternatives to metals for IR plasmonics [31]. Their plasma frequency can be tuned chemically, optically, or electrically across a broad range. Semiconductor-based hyperbolic metamaterials, made of doped-undoped pairs, can be developed to realize narrowband directional IR emission [98,99] and ultrafast and low power all-optical switching [100]. Doped metal oxides have the advantage of visible transparency, making them compatible materials for spacecraft cooling and thermal camouflage [11,101]. 2D materials with exceptional electrical and optical properties are another attractive category in IR plasmonics. Graphene, as the most famous member of this group, can support guided plasmonic modes in the IR range, where the spectral position of these modes can be effectively tuned by its chemical potential (μ) [33,102–104]. Graphene monolayer-based LFMAs have been realized using the excitation of Tamm plasmons in 1D-PC structures [105–107]. Moreover, the use of distributed Bragg reflector (DBR) in a cavity design, to couple light into the graphene monolayer, has been demonstrated [104]. A similar design strategy can be utilized to achieve LFMA using a monolayer of BP [108]. Due to their high carrier mobility, LFMAs made of these 2D materials coupled with narrow bandgap semiconductors have promising applications in IR photodetector designs [109,110]. Different from graphene, the BP monolayer shows strong in-plane anisotropy, used to design polarization selective absorbers [111]. Moreover, different from common narrow bandgap semiconductors, BP has a tunable bandgap from 2 eV (in monolayer) to 0.3 eV (in bulk). Based on recent work [112], a vertical electric field can tune the bandgap of BP and provide a wide tunability (from 3.7 to 7.7 μm) in its photoluminescence (and consequently absorption peak) spectral response. The last category of non-metallic materials is polar dielectrics. These materials are used to make LFMAs in a wide range spanning from MWIR to FIR [2]. The IR optical response of these materials (such as hBN, SiC, AlN, GaN, GaP, and α-MoO_3) are dominated by highly reflective reststrahlen (RS) bands that are located between the longitudinal and transverse optical phonons. Within these RS bands, light can couple with optical phonons to support surface phonon-polariton (SPhPs) modes. LFMAs made of these polar materials are commonly made in 1D-PC and DBR cavity configurations and have been mainly used to realize coherent monochromatic, and directional thermal emitters [113–115]. The hybrid use of these polar materials with PCMs and graphene can provide tunable IR absorbers to be used in radiative cooling, adaptive thermal camouflage, and modulators [116,117]. Moreover, some of these polar materials including BP, hBN, and α-MoO_3 have strong in-plane and out-of-plane anisotropy. This could be utilized to realize lithography-free polarization converters in the IR region [118].

3. Outlook

In summary, besides the development of low-cost, facile, and extendable routes, material exploration is an essential key to realizing cm-scale high-performance LFMAs. The integration of the right elements with large-scale compatible nanofabrication routes will put this technology one step closer to industrialization. In photoconversion, a deep understanding of hot electron dynamics, exploring new materials with a long hot electron lifetime, synthesis of ultrathin high

Optical Materials EXPRESS

mobility crystalline semiconductors, and the development of designer heterojunctions are some of the key goals to be followed. Spectrally-selective thermal emitters are another area of high interest, due to the lack of cost-effective, narrow-band light sources in the MWIR and LWIR. TPV technology and steam generation could also widen the opportunities for the use of these LFMAs in the green energy industry. The integration of these large-scale compatible designs with microfluidic channels can offer a real-time and label-free detection platform for bio-agents with high sensitivity and reliability.

Disclosures. The authors declare no conflicts of interest.

Data availability. No data were generated or analyzed in the presented research.

References

1. E. Ozbay, "Plasmonics: merging photonics and electronics at nanoscale dimensions," Science **311**(5758), 189–193 (2006).
2. A. Ghobadi, H. Hajian, B. Butun, and E. Ozbay, "Strong light-matter interaction in lithography-free planar metamaterial perfect absorbers," ACS Photonics **5**(11), 4203–4221 (2018).
3. J. Toudert, "Spectrally tailored light-matter interaction in lithography-free functional nanomaterials," Phys. Status Solidi A **217**, 1900677 (2020).
4. Z. Liu, X. Liu, S. Huang, P. Pan, J. Chen, G. Liu, and G. Gu, "Automatically acquired broadband plasmonic-metamaterial black absorber during the metallic film-formation," ACS Appl. Mater. Interfaces **7**(8), 4962–4968 (2015).
5. S. Wang, F. Chen, R. Ji, M. Hou, F. Yi, W. Zheng, T. Zhang, and W. Lu, "Large-area low-cost dielectric perfect absorber by one-step sputtering," Adv. Opt. Mater. **7**, 1801596 (2019).
6. A. Ghobadi, S. A. Dereshgi, H. Hajian, B. Bozok, B. Butun, and E. Ozbay, "Ultra-broadband, wide angle absorber utilizing metal insulator multilayers stack with a multi- thickness metal surface texture," Sci. Rep. **7**(1), 4755 (2017).
7. A. Ghobadi, H. Hajian, S. A. Dereshgi, B. Bozok, B. Butun, and E. Ozbay, "Disordered nanohole patterns in metal-insulator multilayer for ultra-broadband light absorption: atomic layer deposition for lithography free highly repeatable large scale multilayer growth," Sci. Rep. **7**(1), 1–10 (2017).
8. A. Ghobadi, H. Hajian, A. R. Rashed, B. Butun, and E. Ozbay, "Tuning the metal filling fraction in metal-insulator-metal ultra-broadband perfect absorbers to maximize the absorption bandwidth," Photonics Res. **6**(3), 168–176 (2018).
9. A. Barranco, A. Borras, A. R. Gonzalez-Elipe, and A. Palmero, "Perspectives on oblique angle deposition of thin films: From fundamentals to devices," Prog. Mater. Sci. **76**, 59–153 (2016).
10. Y. He, J. Fu, and Y. Zhao, "Oblique angle deposition and its applications in plasmonics," Front. Phys. **9**(1), 47–59 (2014).
11. D. U. Yildirim, A. Ghobadi, M. C. Soydan, O. Atesal, A. Toprak, M. D. Caliskan, and E. Ozbay, "Disordered and Densely Packed ITO Nanorods as an Excellent Lithography-Free Optical Solar Reflector Metasurface," ACS Photonics **6**(7), 1812–1822 (2019).
12. Z. Eftekhari, A. Ghobadi, and E. Ozbay, "Lithography-free disordered metal–insulator–metal nanoantennas for colorimetric sensing," Opt. Lett. **45**(24), 6719 (2020).
13. Z. Eftekhari, A. Ghobadi, M. C. Soydan, D. U. Yildirim, N. Cinel, and E. Ozbay, "Strong light emission from a defective hexagonal boron nitride monolayer coupled to near-touching random plasmonic nanounits," Opt. Lett. **46**(7), 1664 (2021).
14. M. C. Soydan, A. Ghobadi, D. U. Yildirim, V. B. Erturk, and E. Ozbay, "Deep subwavelength light confinement in disordered bismuth nanorods as a linearly thermal-tunable metamaterial," Phys. Status Solidi RRL **14**, 2000066 (2020).
15. J. E. Melzer and E. McLeod, "3D Nanophotonic device fabrication using discrete components," Nanophotonics **9**(6), 1373–1390 (2020).
16. L. Shen, C. He, J. Qiu, S. M. Lee, A. Kalita, S. B. Cronin, M. P. Stoykovich, and J. Yoon, "Nanostructured silicon photocathodes for solar water splitting patterned by the self-assembly of lamellar block copolymers," ACS Appl. Mater. Interfaces **7**(47), 26043–26049 (2015).
17. X. Ruan, W. Dai, W. Wang, C. Ou, Q. Xu, Z. Zhou, Z. Wen, C. Liu, J. Hao, Z. Guan, and H. Xu, "Ultrathin, broadband, omnidirectional, and polarization-independent infrared absorber using all-dielectric refractory materials," Nanophotonics **10**(6), 1683–1690 (2021).
18. H. Robatjazi, S. M. Bahauddin, L. H. Macfarlan, S. Fu, and I. Thomann, "Ultrathin AAO membrane as a generic template for sub-100 nm nanostructure fabrication," Chem. Mater. **28**(13), 4546–4553 (2016).
19. U. T. D. Thuy, N. T. Thuy, N. T. Tung, E. Janssens, and N. Q. Liem, "Large-area cost-effective lithography-free infrared metasurface absorbers for molecular detection," APL Mater. **7**(7), 071102 (2019).
20. J. Rensberg, Y. Zhou, S. Richter, C. Wan, S. Zhang, P. Schöppe, R. Schmidt-grund, S. Ramanathan, F. Capasso, M. A. Kats, and C. Ronning, "Epsilon-Near-Zero Substrate Engineering for Ultrathin-Film Perfect Absorbers," Phys. Rev. Lett. **8**(1), 014009 (2017).

21. J. W. Cleary, N. Nader, K. D. Leedy, and R. Soref, "Tunable short- to mid-infrared perfectly absorbing thin films utilizing conductive zinc oxide on metal," Opt. Mater. Express **5**(9), 1898 (2015).
22. M. Sakamoto, T. Kawawaki, M. Kimura, T. Yoshinaga, J. J. M. Vequizo, H. Matsunaga, C. S. K. Ranasinghe, A. Yamakata, H. Matsuzaki, A. Furube, and T. Teranishi, "Clear and transparent nanocrystals for infrared-responsive carrier transfer," Nat. Commun. **10**(1), 1–7 (2019).
23. A. Cleri, J. Tomko, K. Quiambao-Tomko, M. V. Imperatore, Y. Zhu, J. R. Nolen, J. Nordlander, J. D. Caldwell, Z. Mao, N. C. Giebink, K. P. Kelley, E. L. Runnerstrom, P. E. Hopkins, and J. P. Maria, "Mid-wave to near-IR optoelectronic properties and epsilon-near-zero behavior in indium-doped cadmium oxide," Phys. Rev. Mater. **5**(3), 035202 (2021).
24. K. P. Kelley, E. L. Runnerstrom, E. Sachet, C. T. Shelton, E. D. Grimley, A. Klump, J. M. Lebeau, Z. Sitar, J. Y. Suen, W. J. Padilla, and J. P. Maria, "Multiple epsilon-near-zero resonances in multilayered cadmium oxide: designing metamaterial-like optical properties in monolithic materials," ACS Photonics **6**(5), 1139–1145 (2019).
25. E. L. Runnerstrom, A. Bergerud, A. Agrawal, R. W. Johns, C. J. Dahlman, A. Singh, S. M. Selbach, and D. J. Milliron, "Defect engineering in plasmonic metal oxide nanocrystals," Nano Lett. **16**(5), 3390–3398 (2016).
26. G. V. Naik, V. M. Shalaev, and A. Boltasseva, "Alternative plasmonic materials: beyond gold and silver," Adv. Mater. **25**(24), 3264–3294 (2013).
27. G. V. Naik, J. Kim, and A. Boltasseva, "Oxides and nitrides as alternative plasmonic materials in the optical range [Invited]," Opt. Mater. Express **1**(6), 1090–1099 (2011).
28. A. Shabani, M. Tsegay Korsa, S. Petersen, M. Khazaei Nezhad, Y. Kumar Mishra, and J. Adam, "Zirconium nitride: optical properties of an emerging intermetallic for plasmonic applications," Adv. Photonics Res. **2**(11), 2100178 (2021).
29. P. K. B. Palomaki, E. M. Miller, and N. R. Neale, "Control of plasmonic and interband transitions in colloidal indium nitride nanocrystals," J. Am. Chem. Soc. **135**(38), 14142–14150 (2013).
30. H. Shen, L. Yang, Y. Jin, and S. He, "Perfect mid-infrared dual-band optical absorption realized by a simple lithography-free polar dielectric/metal double-layer nanostructure," Opt. Express **28**(21), 31414 (2020).
31. T. Taliercio and P. Biagioni, "Semiconductor infrared plasmonics," Nanophotonics **8**(6), 949–990 (2019).
32. R. Zhou, S. Yang, Q. Lin, L. Tang, D. Liu, K. Ullah, S. Li, and Y. Zhao, "Recent advances in graphene and black phosphorus nonlinear plasmonics," Nanophotonics **9**(7), 1695–1715 (2020).
33. A. N. Grigorenko, M. Polini, and K. S. Novoselov, "Graphene plasmonics," Nat. Photonics **6**(11), 749–758 (2012).
34. Y. Zhong, S. D. Malagari, T. Hamilton, and D. Wasserman, "Review of mid-infrared plasmonic materials," J. Nanophotonics **9**(1), 093791 (2015).
35. C. Ji, K. T. Lee, T. Xu, J. Zhou, H. J. Park, and L. J. Guo, "Engineering Light at the nanoscale: structural color filters and broadband perfect absorbers," Adv. Opt. Mater. **5**, 1700368 (2017).
36. A. C. Kosger, A. Ghobadi, A. R. Rashed, H. Caglayan, and E. Ozbay, "Generation of additive colors with near unity amplitude using a multilayer tandem Fabry–Perot cavity," Opt. Lett. **46**(14), 3464 (2021).
37. A. Ghobadi, H. Hajian, M. Gokbayrak, B. Butun, and E. Ozbay, "Bismuth-based metamaterials: From narrowband reflective color filter to extremely broadband near perfect absorber," Nanophotonics **8**(5), 823–832 (2019).
38. Z. Yang, Y. Zhou, Y. Chen, Y. Wang, P. Dai, Z. Zhang, and H. Duan, "Reflective color filters and monolithic color printing based on asymmetric Fabry–Perot cavities using nickel as a broadband absorber," Adv. Opt. Mater. **4**(8), 1196–1202 (2016).
39. S. Daqiqeh Rezaei, J. Ho, T. Wang, J. K. W. Yang, and S. Ramakrishna, "Direct color printing with an electron beam," Nano Lett. **20**(6), 4422–4429 (2020).
40. J. Lee, J. Kim, and M. Lee, "High-purity reflective color filters based on thin film cavities embedded with an ultrathin $Ge_2Sb_2Te_5$ absorption layer," Nanoscale Adv. **2**(10), 4930–4937 (2020).
41. F. Liu, H. Shi, X. Zhu, P. Dai, Z. Lin, Y. Long, Z. Xie, Y. Zhou, and H. Duan, "Tunable reflective color filters based on asymmetric Fabry–Perot cavities employing ultrathin $Ge_2Sb_2Te_5$ as a broadband absorber," Appl. Opt. **57**(30), 9040 (2018).
42. Q. He, N. Youngblood, Z. Cheng, X. Miao, and H. Bhaskaran, "Dynamically tunable transmissive color filters using ultra-thin phase change materials," Opt. Express **28**(26), 39841 (2020).
43. F. Z. Shu, F. F. Yu, R. W. Peng, Y. Y. Zhu, B. Xiong, R. H. Fan, Z. H. Wang, Y. Liu, and M. Wang, "Dynamic plasmonic color generation based on phase transition of vanadium dioxide," Adv. Opt. Mater. **6**, 1700939 (2018).
44. H. Liu, W. Dong, H. Wang, L. Lu, Q. Ruan, Y. S. Tan, R. E. Simpson, and J. K. W. Yang, "Rewritable color nanoprints in antimony trisulfide films," Sci. Adv. **6**(51), 1–8 (2020).
45. Z. Cheng, T. Milne, P. Salter, J. S. Kim, S. Humphrey, M. Booth, and H. Bhaskaran, "Antimony thin films demonstrate programmable optical nonlinearity," Sci. Adv. **7**(1), 1–10 (2021).
46. T. J. Palinski, A. Tadimety, I. Trase, B. E. Vyhnalek, G. W. Hunter, E. Garmire, and J. X. J. Zhang, "Vibrant reflective sensors with percolation film Fabry-Pérot nanocavities," Opt. Express **29**(16), 25000 (2021).
47. J. Zhang, D. Wang, Y. Ying, H. Zhou, X. Liu, X. Hu, Y. Chen, Q. Li, X. Zhang, and M. Qiu, "Grayscale-patterned metal-hydrogel-metal microscavity for dynamic multi-color display," Nanophotonics **10**(16), 4125–4131 (2021).
48. S. Chervinskii, I. Issah, M. Lahikainen, A. R. Rashed, K. Kuntze, A. Priimagi, and H. Caglayan, "Humidity- and temperature-tunable metal–hydrogel–metal reflective filters," ACS Appl. Mater. Interfaces **13**(42), 50564–50572 (2021).

Optical Materials EXPRESS

49. M. Serhatlioglu, S. Ayas, N. Biyikli, A. Dana, and M. E. Solmaz, "Perfectly absorbing ultra thin interference coatings for hydrogen sensing," Opt. Lett. **41**(8), 1724 (2016).
50. S. Ayas, G. Bakan, E. Ozgur, K. Celebi, G. Torunoglu, and A. Dana, "Colorimetric detection of ultrathin dielectrics on strong interference coatings," Opt. Lett. **43**(6), 1379 (2018).
51. G. Qiu, Z. Gai, Y. Tao, J. Schmitt, G. A. Kullak-Ublick, and J. Wang, "Dual-functional plasmonic photothermal biosensors for highly accurate severe acute respiratory syndrome coronavirus 2 detection," ACS Nano **14**(5), 5268–5277 (2020).
52. K. Yao, R. Toole, P. Basnet, and Y. Zhao, "Highly sensitive double-layered nanorod array gas sensors prepared by oblique angle deposition," Appl. Phys. Lett. **104**(7), 073110 (2014).
53. X. Li, D. Xiao, and Z. Zhang, "Landau damping of quantum plasmons in metal nanostructures," New J. Phys. **15**(2), 023011 (2013).
54. T. P. White and K. R. Catchpole, "Plasmon-enhanced internal photoemission for photovoltaics: theoretical efficiency limits," Appl. Phys. Lett. **101**(7), 073905 (2012).
55. M. W. Knight, N. S. King, L. Liu, H. O. Everitt, P. Nordlander, and N. J. Halas, "Aluminum for plasmonics," ACS Nano **8**(1), 834–840 (2014).
56. L. Zhou, C. Zhang, M. J. McClain, A. Manjavacas, C. M. Krauter, S. Tian, F. Berg, H. O. Everitt, E. A. Carter, P. Nordlander, and N. J. Halas, "Aluminum nanocrystals as a plasmonic photocatalyst for hydrogen dissociation," Nano Lett. **16**(2), 1478–1484 (2016).
57. M. J. McClain, A. E. Schlather, E. Ringe, N. S. King, L. Liu, A. Manjavacas, M. W. Knight, I. Kumar, K. H. Whitmire, H. O. Everitt, P. Nordlander, and N. J. Halas, "Aluminum nanocrystals," Nano Lett. **15**(4), 2751–2755 (2015).
58. M. A. Noginov, L. Gu, J. Livenere, G. Zhu, A. K. Pradhan, R. Mundle, M. Bahoura, Y. A. Barnakov, and V. A. Podolskiy, "Transparent conductive oxides: plasmonic materials for telecom wavelengths," Appl. Phys. Lett. **99**(2), 021101–4 (2011).
59. A. Calzolari, A. Ruini, and A. Catellani, "Transparent conductive oxides as near-IR plasmonic materials: the case of Al-doped ZnO derivatives," ACS Photonics **1**(8), 703–709 (2014).
60. A. Habib, F. Florio, and R. Sundararaman, "Hot carrier dynamics in plasmonic transition metal nitrides," J. Opt. **20**(6), 064001 (2018).
61. U. Guler, V. M. Shalaev, and A. Boltasseva, "Nanoparticle plasmonics: going practical with transition metal nitrides," Mater. Today **18**(4), 227–237 (2015).
62. F. Scotognella, G. Della Valle, A. R. Srimath Kandada, M. Zavelani-Rossi, S. Longhi, G. Lanzani, and F. Tassone, "Plasmonics in heavily-doped semiconductor nanocrystals," Eur. Phys. J. B **86**(4), 154 (2013).
63. F. B. Barho, F. Gonzalez-Posada, M. J. Milla, M. Bomers, L. Cerutti, E. Tournié, and T. Taliercio, "Highly doped semiconductor plasmonic nanoantenna arrays for polarization selective broadband surface-enhanced infrared absorption spectroscopy of vanillin," Nanophotonics **7**(2), 507–516 (2017).
64. I. Kriegel, F. Scotognella, and L. Manna, "Plasmonic doped semiconductor nanocrystals: properties, fabrication, applications and perspectives," Phys. Rep. **674**, 1–52 (2017).
65. T. G. U. Ghobadi, A. Ghobadi, E. Ozbay, and F. Karadas, "Strategies for plasmonic hot-electron-driven photoelectrochemical water splitting," ChemPhotoChem **2**(3), 161–182 (2018).
66. E. Rephaeli and S. Fan, "Absorber and emitter for solar thermo-photovoltaic systems to achieve efficiency exceeding the Shockley-Queisser limit," Opt. Express **17**(17), 15145–15159 (2009).
67. S. M. Fu, Y. K. Zhong, M. H. Tu, B. R. Chen, and A. Lin, "A fully functionalized metamaterial perfect absorber with simple design and implementation," Sci. Rep. **6**(1), 36244 (2016).
68. L. Zhou, Y. Tan, D. Ji, B. Zhu, P. Zhang, J. Xu, Q. Gan, Z. Yu, and J. Zhu, "Self-assembly of highly efficient, broadband plasmonic absorbers for solar steam generation," Sci. Adv. **2**(4), e1501227 (2016).
69. A. Ghobadi, T. G. Ulusoy Ghobadi, F. Karadas, and E. Ozbay, "Semiconductor thin film based metasurfaces and metamaterials for photovoltaic and photoelectrochemical water splitting applications," Adv. Opt. Mater. **7**(14), 1900028 (2019).
70. E. D. Palik, *Handbook of Optical Constants of Solids*. Vol. 3 (Academic, 1998).
71. M. A. Kats, R. Blanchard, P. Genevet, and F. Capasso, "Nanometre optical coatings based on strong interference effects in highly absorbing media," Nat. Mater. **12**(1), 20–24 (2013).
72. S. Fan and X. Zheng, "High-performance ultrathin BiVO4 photoanode on textured polydimethylsiloxane substrates for solar water splitting," ACS Energy Lett. **1**(1), 68–75 (2016).
73. M. Rebello, S. Dias, C. Gong, Z. A. Benson, and M. S. Leite, "Lithography-free, omnidirectional, CMOS-compatible AlCu alloys for thin-film superabsorbers," Adv. Opt. Mater. **6**(2), 1700830 (2018).
74. D. Liu, H. Yu, Z. Yang, and Y. Duan, "Ultrathin planar broadband absorber through effective medium design," Nano Res. **9**(8), 2354–2363 (2016).
75. Q. Li, K. Du, K. Mao, X. Fang, D. Zhao, H. Ye, and M. Qiu, "Transmission enhancement based on strong interference in metal- semiconductor layered film for energy harvesting," Sci. Rep. **6**(1), 29195 (2016).
76. D. Liu, H. Yu, Y. Duan, Q. Li, and Y. Xuan, "New insight into the angle insensitivity of ultrathin planar optical absorbers for broadband solar energy harvesting," Sci. Rep. **6**(1), 32515 (2016).
77. H. Dotan, O. Kfir, E. Sharlin, O. Blank, M. Gross, I. Dumchin, G. Ankonina, and A. Rothschild, "Resonant light trapping in ultrathin films for water splitting," Nat. Mater. **12**(2), 158–164 (2013).

Optical Materials EXPRESS

78. V. Steenhoff, M. Theuring, M. Vehse, and K. Von Maydell, "Ultrathin resonant-cavity-enhanced solar cells with amorphous germanium absorbers," Adv. Opt. Mater. **3**(2), 182–186 (2015).
79. Z. Xia, H. Song, M. Kim, M. Zhou, T. Chang, D. Liu, X. Yin, K. Xiong, H. Mi, X. Wang, F. Xia, Z. Yu, Z. J. Ma, and Q. Gan, "Single-crystalline germanium nanomembrane photodetectors on foreign nanocavities," Sci. Adv. **3**(7), 1–9 (2017).
80. I. A. Digdaya, B. J. Trześniewski, G. W. P. Adhyaksa, E. C. Garnett, and W. A. Smith, "General considerations for improving photovoltage in metal−insulator−semiconductor photoanodes," J. Phys. Chem. C **122**(10), 5462–5471 (2018).
81. J. Zheng, R. A. Barton, and D. Englund, "Broadband coherent absorption in chirped-planar-dielectric cavities for 2D-material-based photovoltaics and photodetectors," ACS Photonics **1**(9), 768–774 (2014).
82. H. Lu, X. Gan, D. Mao, Y. Fan, D. Yang, and J. Zhao, "Nearly perfect absorption of light in monolayer molybdenum disulfide supported by multilayer structures," Opt. Express **25**(18), 21630–21636 (2017).
83. J. D. Ryckman, "Random coherent perfect absorption with 2D atomic materials mediated by Anderson localization," ACS Photonics **5**(2), 574–580 (2018).
84. A. Kay, B. Scherrer, Y. Piekner, K. D. Malviya, D. A. Grave, H. Dotan, and A. Rothschild, "Film flip and transfer process to enhance light harvesting in ultrathin absorber films on specular back-reflectors," Adv. Mater. **30**, 1802781 (2018).
85. Y. Piekner, H. Dotan, A. Tsyganok, K. Deo Malviya, D. A. Grave, O. Kfir, and A. Rothschild, "Implementing strong interference in ultrathin film top absorbers for tandem solar cells," ACS Photonics **5**(12), 5068–5078 (2018).
86. J. Toudert, R. Serna, M. G. Pardo, N. Ramos, R. J. Peláez, and B. Maté, "Mid-to-far infrared tunable perfect absorption by a sub - λ/100 nanofilm in a fractal phasor resonant cavity," Opt. Express **26**(26), 34043 (2018).
87. M. C. Soydan, A. Ghobadi, D. U. Yildirim, E. S. Duman, A. Bek, V. B. Erturk, and E. Ozbay, "Lithography-free random bismuth nanostructures for full solar spectrum harvesting and mid-infrared sensing," Adv. Opt. Mater. **8**(4), 1901203 (2020).
88. H. Peng, Y. Luo, X. Ying, Y. Pu, Y. Jiang, J. Xu, and Z. Liu, "Broadband and highly absorbing multilayer structure in mid-infrared," Appl. Opt. **55**(31), 8833–8837 (2016).
89. X. Liu, Z. Li, Z. Wen, M. Wu, J. Lu, X. Chen, X. Zhao, T. Wang, R. Ji, Y. Zhang, L. Sun, B. Zhang, H. Xu, J. Zhou, J. Hao, S. Wang, X. Chen, N. Dai, W. Lu, and X. Shen, "Large-area, lithography-free, narrow-band and highly directional thermal emitter," Nanoscale **11**(42), 19742–19750 (2019).
90. M. Li, D. Liu, H. Cheng, L. Peng, and M. Zu, "Manipulating metals for adaptive thermal camouflage," Sci. Adv. **6**(22), 1–11 (2020).
91. L. Peng, D. Liu, H. Cheng, S. Zhou, and M. Zu, "A multilayer film based selective thermal emitter for infrared stealth technology," Adv. Opt. Mater. **6**(23), 1801006 (2018).
92. R. Hu, W. Xi, Y. Liu, K. Tang, J. Song, X. Luo, J. Wu, and C. W. Qiu, "Thermal camouflaging metamaterials," Mater. Today **45**, 120–141 (2021).
93. H. Zhu, Q. Li, C. Tao, Y. Hong, Z. Xu, W. Shen, S. Kaur, P. Ghosh, and M. Qiu, "Multispectral camouflage for infrared, visible, lasers and microwave with radiative cooling," Nat. Commun. **12**(1), 1–8 (2021).
94. Y. Qu, Q. Li, L. Cai, M. Pan, P. Ghosh, K. Du, and M. Qiu, "Thermal camouflage based on the phase-changing material GST," Light: Sci. Appl. **7**(1), 1–10 (2018).
95. A. Tittl, A. U. Michel, M. Schäferling, X. Yin, B. Gholipour, L. Cui, M. Wuttig, T. Taubner, F. Neubrech, and H. Giessen, "A switchable mid-infrared plasmonic perfect absorber with multispectral thermal imaging capability," Adv. Mater. **27**(31), 4597–4603 (2015).
96. J. K. Behera, K. Liu, M. Lian, and T. Cao, "A reconfigurable hyperbolic metamaterial perfect absorber," Nanoscale Adv. **3**(6), 1758–1766 (2021).
97. W. J. M. Kort-Kamp, S. Kramadhati, A. K. Azad, M. T. Reiten, and D. A. R. Dalvit, "Passive radiative "thermostat" enabled by phase-change photonic nanostructures," ACS Photonics **5**(11), 4554–4560 (2018).
98. S. Campione, F. Marquier, J. P. Hugonin, A. R. Ellis, J. F. Klem, M. B. Sinclair, and T. S. Luk, "Directional and monochromatic thermal emitter from epsilon-near-zero conditions in semiconductor hyperbolic metamaterials," Sci. Rep. **6**(1), 34746–9 (2016).
99. M. Desouky, A. M. Mahmoud, and M. A. Swillam, "Silicon based mid-IR super absorber using hyperbolic metamaterial," Sci. Rep. **8**(1), 2036 (2018).
100. E. Azmoudeh and S. Farazi, "Ultrafast and low power all-optical switching in the mid-infrared region based on nonlinear highly doped semiconductor hyperbolic metamaterials," Opt. Express **29**(9), 13504 (2021).
101. K. Sun, C. A. Riedel, Y. Wang, A. Urbani, M. Simeoni, S. Mengali, M. Zalkovskij, B. Bilenberg, C. H. De Groot, and O. L. Muskens, "Metasurface optical solar reflectors using AZO transparent conducting oxides for radiative cooling of spacecraft," ACS Photonics **5**(2), 495–501 (2018).
102. K. S. Novoselov, A. K. Geim, S. V. Morozov, D. Jiang, Y. Zhang, S. V. Dubonos, I. V. Grigorieva, and A. A. Firsov, "Electric field effect in atomically thin carbon films," Science **306**(5696), 666–669 (2004).
103. T. Low and P. Avouris, "Graphene plasmonics for terahertz to mid-infrared applications," ACS Nano **8**(2), 1086–1101 (2014).
104. X. Wang, X. Jiang, Q. You, J. Guo, X. Dai, and Y. Xiang, "Tunable and multichannel terahertz perfect absorber due to Tamm surface plasmons with graphene," Photonic Res. **5**(6), 536–542 (2017).

Optical Materials EXPRESS

105. Y. Chang, C. Liu, C. Liu, S. Zhang, S. R. Marder, E. E. Narimanov, Z. Zhong, and T. B. Norris, "Realization of mid-infrared graphene hyperbolic metamaterials," Nat. Commun. **7**(1), 10568 (2016).
106. M. A. K. Othman, C. Guclu, and F. Capolino, "Graphene-based tunable hyperbolic metamaterials and enhanced near-field absorption," Opt. Express **21**(6), 7614–7632 (2013).
107. R. Ning, S. Liu, H. Zhang, B. Bian, and X. Kong, "Tunable absorption in graphene-based hyperbolic metamaterials for mid-infrared range," Phys. B **457**, 144–148 (2015).
108. D. Dong, Y. Liu, Y. Fei, Y. Fan, J. Li, Y. Feng, and Y. Fu, "Designing a nearly perfect infrared absorber in monolayer black phosphorus," Appl. Opt. **58**(14), 3862 (2019).
109. X. Yu, Y. Li, X. Hu, D. Zhang, Y. Tao, Z. Liu, Y. He, M. A. Haque, Z. Liu, T. Wu, and Q. J. Wang, "Narrow bandgap oxide nanoparticles coupled with graphene for high performance mid-infrared photodetection," Nat. Commun. **9**(1), 1–8 (2018).
110. C. Lan, Z. Shi, R. Cao, C. Li, and H. Zhang, "2D materials beyond graphene toward Si integrated infrared optoelectronic devices," Nanoscale **12**(22), 11784–11807 (2020).
111. N. S. Azar, J. Bullock, S. Balendhran, H. Kim, A. Javey, and K. B. Crozier, "Light-matter interaction enhancement in anisotropic 2D black phosphorus via polarization-tailoring nano-optics," ACS Photonics **8**(4), 1120–1128 (2021).
112. C. Chen, X. Lu, B. Deng, X. Chen, Q. Guo, C. Li, C. Ma, S. Yuan, E. Sung, K. Watanabe, T. Taniguchi, L. Yang, and F. Xia, "Widely tunable mid-infrared light emission in thin-film black phosphorus," Sci. Adv. **6**(7), 1–8 (2020).
113. B. J. Lee, C. J. Fu, and Z. M. Zhang, "Coherent thermal emission from one-dimensional photonic crystals," Appl. Phys. Lett. **87**(7), 071904 (2005).
114. B. J. Lee and Z. M. Zhang, "Coherent thermal emission from modified periodic multilayer structures," J. Heat Transfer **129**(1), 17–26 (2007).
115. H. Hajian, A. Ghobadi, B. Butun, and E. Ozbay, "Nearly perfect resonant absorption and coherent thermal emission by hBN-based photonic crystals," Opt. Express **25**(25), 31970–31987 (2017).
116. S. Abedini Dereshgi, M. C. Larciprete, M. Centini, A. A. Murthy, K. Tang, J. Wu, V. P. Dravid, and K. Aydin, "Tuning of optical phonons in α-MoO_3 –VO_2 multilayers," ACS Appl. Mater. Interfaces **13**(41), 48981–48987 (2021).
117. K. Shi, F. Bao, and S. He, "Enhanced near-field thermal radiation based on multilayer graphene-hBN heterostructures," ACS Photonics **4**(4), 971–978 (2017).
118. S. Abedini Dereshgi, T. G. Folland, A. A. Murthy, X. Song, I. Tanriover, V. P. Dravid, J. D. Caldwell, and K. Aydin, "Lithography-free IR polarization converters via orthogonal in-plane phonons in α-MoO_3 flakes," Nat. Commun. **11**(1), 5771 (2020).